epl A Letters Journal Exploring the Frontiers of Physics

February 2010

EPL, **89** (2010) 34002
doi: 10.1209/0295-5075/89/34002

www.epljournal.org

The packing properties of superellipsoids

G. W. Delaney[(a)] and P. W. Cleary

CSIRO Mathematical and Information Sciences - Private Bag 33, Clayton South, Vic, 3168, Australia

received 28 October 2009; accepted in final form 18 January 2010
published online 18 February 2010

PACS 45.70.-n – Granular systems
PACS 61.43.Bn – Structural modeling: serial-addition models, computer simulation
PACS 61.20.-p – Structure of liquids

Abstract – We investigate the properties of packings of frictionless non-spherical particles utilizing a dynamic particle expansion technique. We employ superquadric particles (superellipsoids), which allows us to explore how a broad range of particle shapes affect both the macroscopic and the local configurational properties of the system. We smoothly transition from spherical particles possessing only translational degrees of freedom to large aspect ratio non-spherical grains where rotational degrees of freedom are highly important. We demonstrate that the degree of anisotropy and local surface curvature of the particles have a profound effect on their packing properties, determining whether a random or an ordered packing is readily formed.

Investigations of granular packings is a recurrent theme in engineering and the physical sciences [1]. Begun with the study of monodisperse sphere packings by Bernal and then Scott [2,3], this work has influenced broad research areas, from understanding liquids and jamming, to unlocking the secrets of transitions in glasses and other more exotic materials [4,5]. Collections of granular particles show many different behaviors, transitioning from fluid-like behavior at low densities to rigid solid-like behavior as the density increases [1]. A key transition is found at the Random Close Packing limit, where the system jams in its most dense disordered state. This limit has been well established for spheres at a density $\Phi \simeq 0.64$ [2] and occurs at the same density as the Maximally Random Jammed (MRJ) state, which for simulations of frictionless particles corresponds to the least ordered among all the jammed packings [6]. Williams and Philipse demonstrated that introducing asphericity to the particle shape can increase the density in random packings above that of spheres, finding a maximum packing fraction $\Phi \simeq 0.695$ for spherocylinders with aspect ratio $\alpha \simeq 0.71$ [7]. Ellipsoids follow a similar trend to that observed for spherocylinders, with maximum packing fractions found around $\Phi \simeq 0.735$ for fully aspherical ellipsoids [8]. Ellipses in 2D also show this trend where for dense random packings maximum densities around $\Phi \simeq 0.895$ are found [9] and in the Rotational Random Apollonian Packing model where the packing efficiency exponent exhibits a peak at around $\alpha \simeq 0.5$ [10]. At densities above those of random packings, clear signs of ordering emerge. This can range from local crystallization to other forms of ordering including nematic phases, where there is orientational ordering without positional ordering, smectic phases where grains form ordered layers and cubatic phases where the system has three distinct axes about which the grains order [11,12]. The denser crystalline packings are also of wide applicability to problems in chemistry and in understanding granular media. The Kepler conjecture for the maximal packing of spherical grains has just recently been proved [13]. Ordered packings of non-spherical grains have also been investigated, with certain families of Bravais lattice packings being identified as possible maximal packing arrangements for superballs [14].

In this work we will consider how a particular grain's shape affects its tendency to form an ordered or a disordered packing, and how we can relate the properties of a grain shape to the type of ordering observed. We utilize 3D superellipsoids defined by

$$\left(\frac{x}{a}\right)^m + \left(\frac{y}{b}\right)^m + \left(\frac{z}{c}\right)^m = 1, \tag{1}$$

where we refer to m as the shape parameter, and a, b and c are the semi-major axis lengths. For $m = 2$, we recover the general formula for an ellipsoid, while larger values of m generate increasingly cubic shapes (see fig. 1). This gives us the ability to investigate a broad range of particle shapes, smoothly transitioning through a range of surface curvatures and aspect ratios [15]. In this way we can

[(a)] E-mail: gary.delaney@csiro.au

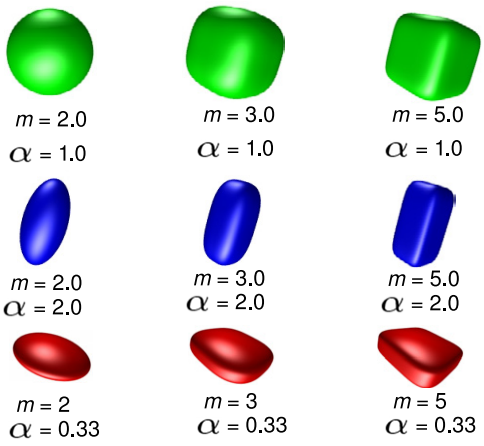

Fig. 1: (Colour on-line) Examples of superellipsoids with shape parameter m and aspect ratio α (major-axis lengths $a = 1, b = 1$ and $c = \alpha$).

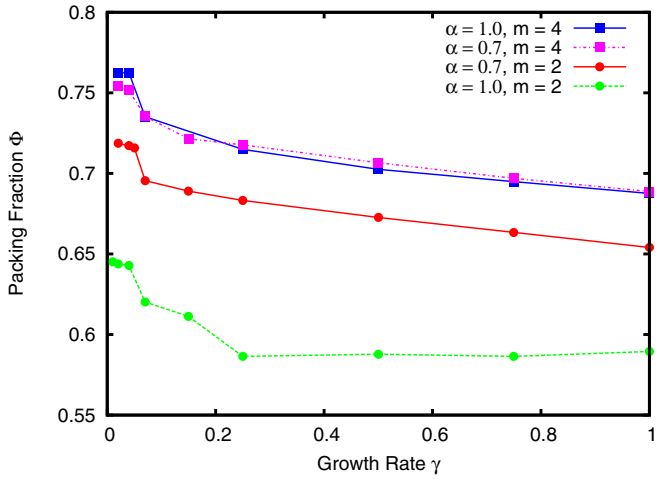

Fig. 2: (Colour on-line) Dependence of packing fraction Φ on the growth rate γ. For spheres ($m = 2$, $\alpha = 1$) and prolate ellipsoids ($m = 2$, α=0.7) the system transitions smoothly to the RCP limit as the growth rate is reduced. For superellipsoids with larger shape parameters ($m = 4$), higher densities and a definite transition to ordered structures is observed at low growth rates.

quantify how the degree of anisotropy of the particle shape affects the packing properties and the effect that regions of low surface curvature have on the packing behavior. Superellipsoids have previously been utilized in large-scale industrial simulations of granular flow, where they have highlighted the important role particle shape plays in the behavior of granular systems [16,17].

We initially seed our simulation with particles in a unit periodic box at random positions and orientations at a low packing fraction ($\Phi < 0.2$). Our particles have unit density and are frictionless. We utilize a fully dynamic linear spring Discrete Element Method (DEM) simulation to model the interaction between particles [18,19]. At each iteration we obtain the contact locations and linear overlaps between particles and hence solve for the forces and torques on each particle. Further details of our DEM technique are given in refs. [16,20,21]. Our simulations proceed by slowly and uniformly increasing the size of the particles at a constant volumetric growth rate γ, while imposing a condition of constant kinetic energy. This is a similar technique as that defined by the Lubachevsky-Stillinger algorithm for hard particles [22]. We utilize a large spring constant to ensure very low inter-particle overlaps of less than $5 \times 10^{-4} d$, where d is the major axis length. The simulation has a well-defined final point where the average overlap diverges sharply as the system jams.

The growth rate γ determines the final packing fraction, consistent with previous studies utilizing dynamic simulations of growing particles [23]. Our technique produces random packings of spheres and ellipsoids ($m = 2$) at the RCP limit for low growth rates (fig. 2). For superellipsoids with larger values of m (increasingly cubic shapes), we also observe an increase in Φ as γ is reduced. However, the system forms substantially denser packings at low growth rates and these packings exhibit clear signs of ordering, with highly ordered arrangements observed for large values of m (see fig. 3). At large deviations from unit aspect ratios we also see the formation of columnar phases (fig. 3(c)).

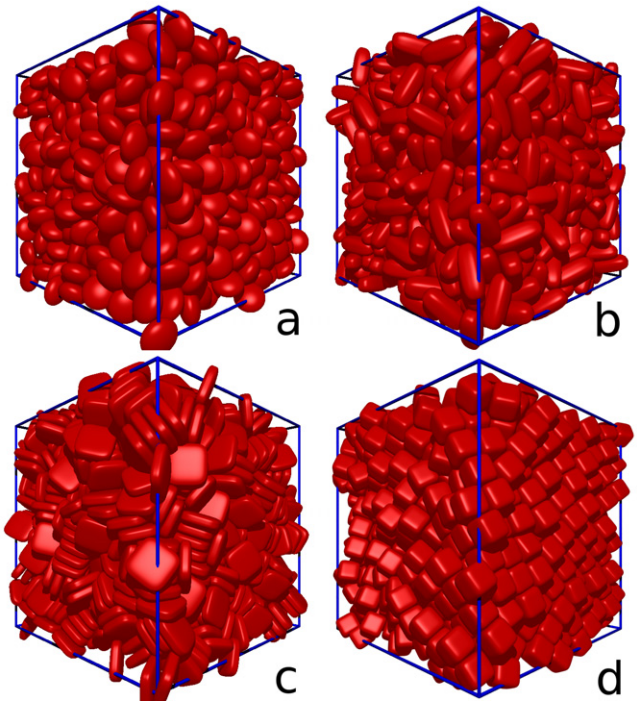

Fig. 3: (Colour on-line) Packings of $N = 1125$ biaxial superellipsoids with $m = 2$ and $\alpha = 0.6$ (a), $m = 3$ and $\alpha = 2.5$ (b), $m = 4$ and $\alpha = 0.3$ (c), $m = 5$ and $\alpha = 1.0$ (d).

These are caused by ordering of the large faces of the oblate grains and are not as readily formed for similar aspect ratios of the prolate grains. This behaviour is similar to what is observed in simulations of cut spheres, where oblate particles were seen to arrange themselves in long columns [24].

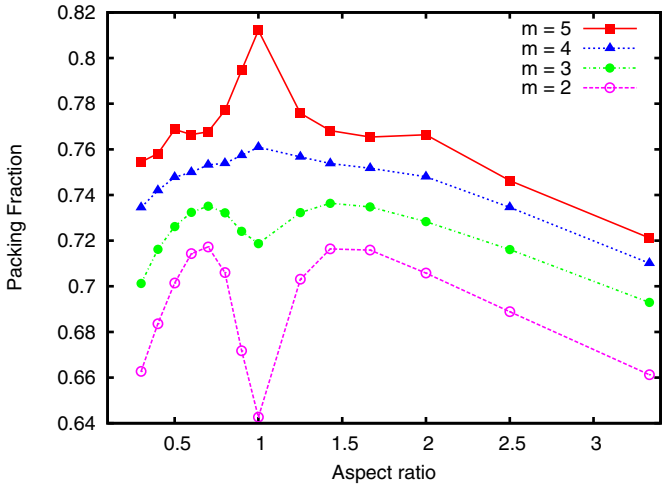

Fig. 4: (Colour on-line) Variation in packing fraction with aspect ratio for superellipsoids with $m = 2$, 3, 4 and 5. All simulations used a growth rate $\gamma = 0.04$.

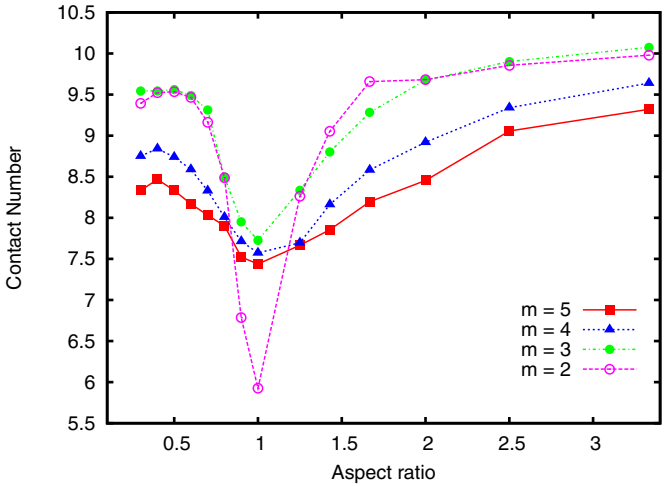

Fig. 5: (Colour on-line) Variation in average contact number $\bar{c}$ with the aspect ratio α of the particles.

Figure 4 shows the variation in packing fraction with the particle's aspect ratio α (corresponding to major-axis lengths $a = 1, b = 1, c = \alpha$) for a growth rate $\gamma = 0.04$. For each particle shape, 5 packings containing $N = 1125$ grains were generated and the data averaged. We consider packings for a very broad range of grain shapes, all generated utilizing the same simulation conditions, allowing us to observe the way in which shape affects how readily ordered *vs.* disordered packings form. This growth rate is sufficiently low to ensure that we generate sphere packings ($m = 2, \alpha = 1$) at the RCP density limit of $\Phi \simeq 0.64$. For ellipsoids ($m = 2$), our technique generates dense disordered packings. These packings are both spatially and orientationally disordered and have densities consistent with those found for the RCP limit in hard particle simulations [23]. For $m = 3$ we observe a very large increase in the density for superballs ($\alpha = 1$) above that of spheres, finding a value of $\Phi \simeq 0.72$. The packing fraction variation at other aspect ratios follows a similar trend to that observed for ellipsoids, with peaks in the packing fraction observed at $\alpha \simeq 0.7$ and $\alpha \simeq 1.5$. For $m = 4$ a very different behavior is observed, with a maximum packing fraction obtained for $\alpha = 1$, with all other aspect ratios having a lower density. A similar behavior is followed for $m = 5$, with a very large $\Phi \simeq 0.815$ found for $\alpha = 1$, that rapidly drops off for non-unit aspect ratios. These denser packings have a high degree of orientational ordering. This is most evident in the case of superballs ($\alpha = 1$), where we can see from fig. 3 that the system forms highly ordered packings, with particles orientational aligned and arranged in ordered layers. As we introduce the effect of aspect ratio we find that the packing fraction decreases rapidly, but signs of ordering remain, such as the columns composed of up to 8 particles observed for $\alpha = 2$ in fig. 3(c).

The average number of particles in contact $\bar{c}$ is a very useful quantity in characterizing granular packings, giving key information on the geometrical properties and the stability of the packing [25,26]. The study of this quantity has its roots in the work of Maxwell [27] and more recently Bennet [28]. The standard "isocounting conjecture" asserts that to constrain a system two contacts per degree of freedom d_f are required ($\bar{c} = 2d_f$) [29]. This has been seen to not be universally applicable to non-spherical particles, in particular for elliptical particles at low aspect ratios a lower $\bar{c}$ is observed [23,29]. Donev *et al.* have however demonstrated that such underconstrained packings can in fact still be jammed [30]. Our ellipsoid packings follow this same trend, with isocounting performing well for spheres ($\bar{c} \simeq 6$), but the contact number varies in a continuous manner towards $\bar{c} \simeq 10$ for large aspect ratio biaxial ellipsoids (see fig. 5). Superballs with $m = 3$ exhibit a large jump in contact number above spheres to $\bar{c} \simeq 7.7$ and then a similar smooth transition toward $\bar{c} \simeq 10$ at high aspect ratios. The structural properties of the packings clearly change as the shape parameter m is increased, with the particles having a high degree of orientational alignment, and a general reduction in the contact numbers found for $m = 4$ and $m = 5$.

To quantify the orientational ordering we employ the orientational alignment tensor $\boldsymbol{Q}$, defined as

$$\boldsymbol{Q}^{\eta\eta} = \frac{1}{N}\sum_{i=1}^{N}\frac{3}{2}\boldsymbol{p}_{\eta}^{(i)} \otimes \boldsymbol{p}_{\eta}^{(i)} - \frac{1}{2}I, \tag{2}$$

where $\boldsymbol{p}_{\eta}$ is a unit column vector pointing along a particular axis η of the superellipsoid, I is the identity matrix and the summation is performed over the N particles in the system. For grains with non-unit aspect ratios ($\alpha \neq 1$) where the major axis is taken to be the $\boldsymbol{z}$-axis, the eigenvectors of $\boldsymbol{Q}$ are composed of the principal nematic director $\boldsymbol{Z}$ and two vectors normal to $\boldsymbol{Z}$. The nematic order parameter S_2 quantifying the degree of orientational ordering is then found from the associated eigenvalue of the nematic director $\boldsymbol{Z}$ [11]. Our packings

have very little of this type of nematic ordering, with $S_2 < 0.1$ for all the grain shapes considered in this letter.

To quantify the type of ordering we observe in our system, let us first consider the case of superballs ($\alpha = 1$, $m > 2$). In this case, each particle's 3 axes are equivalent and so we must take account of this symmetry in determining the degree of orientational ordering in the system. To do this, we separate each of the three axes of each particle into one of three sets $\{\boldsymbol{u}_i\}, \{\boldsymbol{v}_i\}$ and $\{\boldsymbol{w}_i\}$, based on the best alignment of the particle axis with a reference set of axes chosen so as the maximise their overall alignment with all the particle axes [12]. To determine this reference set of axes we consider each set of particle axes as candidates and choose the set that gives the maximum overall alignment for the system. We then form three ordering tensors $\boldsymbol{Q}^{uu}, \boldsymbol{Q}^{vv}$ and $\boldsymbol{Q}^{ww}$, and determine for each its maximum eigenvalue denoted as $\lambda_+^u, \lambda_+^v, \lambda_+^w$ respectively. These eigenvalues identify which of the sets of vectors correspond to the $\boldsymbol{z}$-axes (most aligned), $\boldsymbol{y}$-axes (2nd most aligned) and $\boldsymbol{x}$-axes (least aligned), *e.g.* $\{\boldsymbol{z}_i\} = \{\boldsymbol{u}_i\}$ if λ_+^u is the largest and the corresponding eigenvector represents the $\boldsymbol{Z}$ director vector. We also construct two other orthogonal director vectors. The $\boldsymbol{Y}$ director is found from projecting the eigenvector corresponding to the second largest λ_+ into the plane normal to $\boldsymbol{Z}$. The $\boldsymbol{X}$-axis is then simply the vector normal to $\boldsymbol{Y}$ and $\boldsymbol{Z}$. (Note that in general $\boldsymbol{Y}$and $\boldsymbol{X}$ will be nearly equivalent to the eigenvectors associated with the second and third largest λ_+ eigenvalues.) We then quantify the average uniaxial ordering by

$$S_{\text{avg}} = \frac{2}{3}\left(\boldsymbol{Z}\boldsymbol{Q}^{zz}\boldsymbol{Z} + \boldsymbol{Y}\boldsymbol{Q}^{yy}\boldsymbol{Y} + \boldsymbol{X}\boldsymbol{Q}^{xx}\boldsymbol{X}\right) - 1. \quad (3)$$

This order parameter can also be used for superellipsoids with non-unit aspect ratios ($\alpha \neq 1$), where by considering the three axes to be equivalent it quantifies the degree of face-on-face ordering of the particles. We also determine a biaxial order parameter (quantifying the degree of alignment of the system with the $\boldsymbol{X}$ and $\boldsymbol{Y}$ axes) from

$$S_{\text{biaxial}} = \frac{2}{3}\left(\boldsymbol{X}\boldsymbol{Q}^{xx}\boldsymbol{X} + \boldsymbol{Y}\boldsymbol{Q}^{yy}\boldsymbol{Y} - \boldsymbol{X}\boldsymbol{Q}^{yy}\boldsymbol{X} - \boldsymbol{Y}\boldsymbol{Q}^{xx}\boldsymbol{Y}\right) - 1. \quad (4)$$

In a perfectly aligned system where the three axes of every grain is aligned with one of the 3 directors, $S_{\text{avg}} = 1$ and $S_{\text{biaxial}} = 1$.

Figure 6 shows the variation in the S_{avg} order parameter for a range of shape parameters m and aspect ratios α. We see that as the shape parameter m is increased, we obtain packings with increasing orientational ordering. This ordering is strongest for superballs ($\alpha = 1$) where the high degree of symmetry of the shape aids the ordering effect. Changing α away from unity introduces a higher degree of anisotropy into the particle shape and for large values of m causes a rapid drop off in S_{avg}. This trend correlates with the drop in packing fraction observed in fig. 4. Interestingly, for $m = 5$ and aspect ratios of $\alpha = 0.5$ and 2.0, the orientational ordering and packing density is slightly above the trend. This increase may be due to the ease with which two grains can exactly pack with their shorter sides against one of the longer sides of a third grain. The S_{biaxial} order parameter follows the same trends as observed for S_{avg}, but with consistently lower values observed (fig. 7). The high values of S_{avg} and S_{biaxial} for large m and low α values show that in these shape ranges the system is exhibiting a cubatic-type ordering, with orientational alignment occurring not only with the

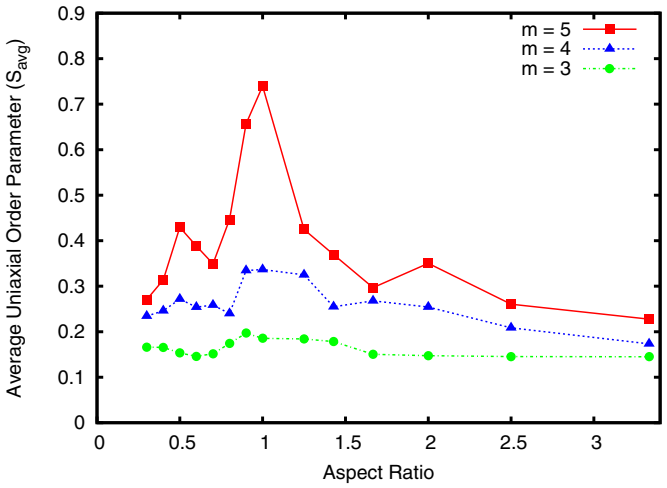

Fig. 6: (Colour on-line) Measurement of the average uniaxial order parameter S_{avg} shows the high degree of orientational ordering for unit aspect ratio superellipsoids at high shape parameters ($m = 5$). This ordering falls off rapidly at moderate aspect ratios. For low shape parameter values ($m = 3$) a considerably reduced degree of ordering is observed.

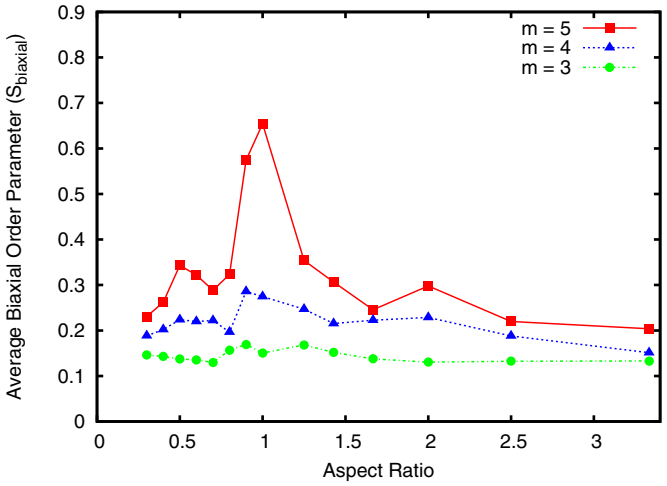

Fig. 7: (Colour on-line) Measurement of the biaxial order parameter S_{biaxial}. This follows a similar trend to that observed for S_{avg}. For high m values and low aspect ratios the system exhibits a high degree of orientationally ordering along three distinct axes.

principal director $\boldsymbol{Z}$ but also along the other two director vectors.

We see that the shape of the particles causes very different final structures to form, covering the entire range from packings with no discernible ordering right up to near crystalline packings. Two key properties of the grain shape determine the packing behaviour, its degree of anisotropy (aspect ratio) and its surface curvature. The large regions of low surface curvature for high m values, readily generate large amounts of face on face inter-grain contacts and thus large amounts of orientational ordering, leading to dense ordered packings. At high m values ($m=4$ and $m=5$), the densest packings are formed by the grains with the highest degree of symmetry ($\alpha=1$) and as we increase the anisotropy of the grain shape by changing the aspect ratio away from unity, we see a rapid drop off in the ordering and the density of the packings falls. Clearly high degrees of symmetry aid ordering effects and the anisotropy reduces the ability of a very ordered packing to form, leading to a decrease in both the density and the orientational ordering. This is contrary to the behavior at low m values ($m=2$ and 3) where predominantly disordered packings are formed and moderate degrees of anisotropy cause an increase in packing fraction.

Understanding the packing properties of different classes of particles is important in many industrial applications from systems where self-assembly is highly desirable, *e.g.*, producing patterned structures, to applications that require dense random granular packings, *e.g.*, the contents of pharmaceutical tablets [31]. Numerical packing models also have applications in particle breakage simulations, where a broken particle needs to be replaced with a packing of daughter particles with a realistic shape and size distribution [16,32]. The results presented here will also have applicability in guiding the development of detailed theoretical models for granular materials that take account of the complexities introduced by grain shape. Progress is already being made in this area with the development of exactly solvable 2D rectangular lattice models for shaken sand grains [33] and models of granular columns that incorporate rotational degrees of freedom of the grains [34,35].

In future studies we will examine packings of fully aspherical superellipsoids with three independent axis lengths and polydisperse packings.

REFERENCES

[1] Aste T. and Weaire D., *The Pursuit of Perfect Packing* 2nd edition (Taylor & Francis, Boca Raton, Fla.) 2008.
[2] Bernal J. D. and Mason J., *Nature*, **188** (1960) 910.
[3] Scott G. D., Knight K. R., Bernal J. D. and Mason J., *Nature*, **194** (1962) 956.
[4] OHern C. S., Silbert L. E., Liu A. J. and Nagel S. R., *Phys. Rev. E*, **68** (2003) 011306.
[5] Liu A. J. and Nagel S. R., *Nature*, **396** (1998) 21.
[6] Torquato S., Truskett T. M. and Debenedetti P. G., *Phys. Rev. Lett.*, **84** (2000) 2064.
[7] Williams S. R. and Philipse A. P., *Phys. Rev. E*, **67** (2003) 051301.
[8] Donev A., Cisse I., Sachs D., Variano E. A., Stillinger F. H., Connelly R., Torquato S. and Chaikin P. M., *Science*, **303** (2004) 990.
[9] Delaney G., Weaire D., Hutzler S. and Murphy S., *Philos. Mag. Lett.*, **85** (2005) 89.
[10] Delaney G. W., Hutzler S. and Aste T., *Phys. Rev. Lett.*, **101** (2008) 120602.
[11] Frenkel D. and Eppenga R., *Phys. Rev. A*, **31** (1985) 1776.
[12] John B. S., Stroock A. and Escobedo F. A., *J Chem. Phys.*, **120** (2004) 9383.
[13] Hales T., *Ann. Math.*, **162** (2005) 1065.
[14] Jiao Y., Stillinger F. H. and Torquato S., *Phys. Rev. E*, **79** (2009) 041309.
[15] Delaney G. W. and Cleary P. W., in *Powders and Grains: Proceedings of the 6th International Conference on Micromechanics of Granular Media, Golden, CO, 13–17 July 2009, AIP Conf. Proc.* **1145** (2009) 837.
[16] Cleary P., *Powder Technol.*, **179** (2008) 144.
[17] Cleary P., Robinson G., Golding M. and Owen P., *Chem. Eng. Sci.*, **63** (2008) 5681.
[18] Cundall P. and Strack O., *Geotechnique*, **29** (1979) 65, 47.
[19] Hutzler S., Delaney G., Weaire D. and MacLeod F., *Am. J. Phys.*, **72** (2004) 1508.
[20] Cleary P. W., *Eng. Comput.*, **21** (2004) 169.
[21] Cleary P., *Miner. Eng.*, **11** (1998) 1061.
[22] Lubachevsky B. D. and Stillinger F. H., *J. Stat. Phys.*, **60** (1990) 561.
[23] Donev A., Torquato S., Stillinger F. H. and Connelly R., *Phys. Rev. E*, **70** (2004) 043301.
[24] Wouterse A., Williams S. R. and Philipse A. P., *J. Phys.: Condens. Matter*, **19** (2007) 406215.
[25] Delaney G., Inagaki S. and Aste T., *Granular Complex Mater.*, **8** (2007) 169.
[26] Aste T., Matteo T. D. and Delaney G. W., in *Powders and Grains: Proceedings of the 6th International Conference on Micromechanics of Granular Media, Golden, CO, 13–17 July 2009, AIP Conf. Proc.* **1145** (2009) 203.
[27] Maxwell J. C., *Philos. Mag.*, **27** (1864) 294.
[28] Bennet C., *J. Appl. Phys.*, **43(6)** (1972) 2727.
[29] Delaney G. W., Weaire D. and Hutzler S., *Europhys. Lett.*, **72** (2005) 990.
[30] Donev A., Connelly R., Stillinger F. H. and Torquato S., *Phys. Rev. E*, **75** (2007) 051304.
[31] Alderborn G. and Nystrom C., *Pharmaceutical Powder Compaction Technology* (Informa Health Care) 1995.
[32] Cleary P. W., *Miner. Eng.*, **14** (2001) 1295.
[33] Stadler P. F., Luck J. M. and Mehta A., *Europhys. Lett.*, **57** (2002) 46.
[34] Luck J. M. and Mehta A., *Eur. Phys. J. B*, **57** (2007) 429.
[35] Mehta A., Barker G. C. and Luck J. M., *Proc. Natl. Acad. Sci. U.S.A.*, **105** (2008) 8244.